Applied Catalysis A: General 455 (2013) 46–57

Contents lists available at SciVerse ScienceDirect

Applied Catalysis A: General

journal homepage: www.elsevier.com/locate/apcata

# High-performance ring-opening catalysts based on iridium-containing zeolite Beta in the hydroconversion of decalin

Dominic Santi[a], Tobias Holl[a], Vincenzo Calemma[b], Jens Weitkamp[a,*]

[a] Institute of Chemical Technology, University of Stuttgart, 70550 Stuttgart, Germany
[b] Eni S.p.A., R&M Division, Via F. Maritano 26, 20097 San Donato Milanese, Italy

ARTICLE INFO

*Article history:*
Received 7 December 2012
Received in revised form 16 January 2013
Accepted 18 January 2013
Available online 8 February 2013

*Keywords:*
Selective ring opening
Open-chain decanes
Ir/Beta
HIPEROCs
Bifunctional catalysis
Hydrogenolysis
Decalin

ABSTRACT

Decalin was converted in a flow-type reactor under a hydrogen pressure of 5.2 MPa on Ir/H,A-Beta zeolite catalysts, where A stands for an alkali metal cation. In one series of catalysts, the Ir content was 3 wt.%, and the nature of A was varied from lithium to cesium. In a second series, the iridium content in Ir/H,Cs-Beta was varied from 1 to 5 wt.%. On some of these catalysts, open-chain decanes (OCDs) were formed with unprecedented selectivities and yields of up to 47 and 44%, respectively. The term "High-Performance Ring-Opening Catalysts" (HIPEROCs) was defined. Evidence is presented for hydrogenolysis on the metal being the main ring-opening mechanism on HIPEROCs. The main function of the Brønsted-acid sites is a mild isomerization of six-membered into five-membered naphthenic rings which are much easier to open by hydrogenolysis. Valuable mechanistic information can be deduced from the carbon-number distributions and the naphthenes vs. alkanes content of the hydrocracked products ($C_9$-).



## 1. Introduction

There has recently been considerable concern about polynuclear aromatic hydrocarbons (PAHs) in diesel fuel, as they have very poor cetane numbers [1], unfavorable cold-flow properties, excessively high densities, a low hydrogen content leading to high specific $CO_2$ emissions, and they are considered to be the main precursors of soot in the tail gas. The conversion of PAH-rich refinery streams, such as light cycle oil (LCO) from fluid catalytic crackers or middle distillate fractions from cokers into hydrogen-rich, environmentally benign blending cuts for diesel fuel continues to be among the challenges of heterogeneous catalysis. The ideal products of such a conversion would be alkanes with the same carbon numbers as the PAH reactants. Such a route would comprise two steps, namely the complete hydrogenation of the PAHs to the corresponding multi-ring naphthenes followed by their selective ring opening to alkanes. Since the hydrogenation of aromatics is often considered as state-of-the-art catalysis, various groups were, within the past 10–15 years, looking in detail at the selective catalytic ring opening of multi-ring naphthenes.

The most widely used model hydrocarbons for such studies seem to be decalin and tetralin, and the catalysts can beclassified as monofunctional acidic (e.g., zeolites in a Brønsted-acid form, $WO_3/Al_2O_3$ [2–4]), monofunctional metallic (mostly iridium or platinum on non-acidic supports [4–6]), or bifunctional (e.g., platinum or iridium on Brønsted-acid forms of zeolites Y, Beta, or mordenite [3,7–18]).

Literature tells that monofunctional acidic catalysts are inappropriate for ring opening of decalin, because they undergo deactivation due to coking, significant amounts of hydrocarbons with more than 10 carbon atoms are formed at elevated conversions, and the yields of ring-opening products are unacceptably low, generally about 10% at most [2–4]. The chemistry of ring opening on such catalysts proceeds via carbocations, either by classical β-scissions or through direct protolytic cracking at a tertiary carbon atom of decalin [2,4].

On monofunctional metallic catalysts ring opening of naphthenes occurs by hydrogenolysis of endocyclic carbon–carbon bonds. Based on Gault's pioneering work with relatively small monocyclic model hydrocarbons, e.g., methylcyclopentane, and $Pt/Al_2O_3$ catalysts with various platinum loadings, three distinct ring-opening mechanisms are usually discerned [19]: (a) the non-selective (or multiplet) mechanism proceeding on highly dispersed platinum and featuring an equal probability for cleavage of all five endocyclic bonds, (b) the selective (or dicarbene) mechanism occurring on poorly dispersed platinum and breaking unsubstituted, i.e., secondary carbon–carbon bonds exclusively, and (c) the partially selective (or metallacyclobutane) mechanism competing

* Corresponding author. Tel.: +49 711 685 64060; fax: +49 711 685 64065.
*E-mail address:* jens.weitkamp@itc.uni-stuttgart.de (J. Weitkamp).

0926-860X/$ – see front matter © 2013 Elsevier B.V. All rights reserved.
http://dx.doi.org/10.1016/j.apcata.2013.01.020

with the selective mechanism in cases when at least one carbon atom is substituted by a methyl group. Iridium was found to open the ring of methylcyclopentane [5,20] and pentylcyclopentane [5,21] according to an almost purely selective mechanism, irrespective of the metal dispersion. By converting a variety of monocyclic naphthenes with up to ten carbon atoms, McVicker et al. [5] and Daage et al. [21] disclosed a number of very interesting features of selective ring opening by hydrogenolysis on iridium. Iridium is much more active in the ring opening of naphthenes than platinum, and it opens five-membered naphthenic rings significantly faster than six-membered rings. It is, nevertheless, capable as well to open six-membered rings, e.g., in methylcyclohexane. If the number of alkyl substituents on the naphthenic ring is increased, e.g., by going from methylcyclohexane to 1,2,4-trimethylcyclohexane, both the rate and the selectivity of ring opening on $Ir/Al_2O_3$ are markedly reduced [5]. Ring opening of monocyclic naphthenes by hydrogenolysis on various mono- and bimetallic catalysts has also been dealt with in several Exxon patents [22–24] showing a considerable industrial interest in the subject. A concept should also be mentioned that has been advanced in Refs. [5,21], viz. the combination of a metal for hydrogenolytic ring opening with a mildly acidic component for isomerization of naphthenes with a six-membered ring into isomers with a five-membered ring which are much more readily opened by hydrogenolysis.

In two very recent studies, the reaction paths of the hydroconversion of decalin over iridium supported on non-acidic carriers, viz. $\gamma$-$Al_2O_3$ [4] and $SiO_2$ [6], were investigated in much detail. Depending on the iridium content of the catalyst (0.5–2.6 wt.%), decalin conversion starts between 250 and 350 °C. There is virtually no skeletal isomerization, direct opening of one six-membered ring rather occurs leading at low conversions almost exclusively to the "direct ring-opening products" 1-methyl-2-propylcyclohexane, 1,2-diethylcyclohexane and butylcyclohexane in a ratio of about 52:35:13 [4,6]. This result nicely confirms that the selective ring-opening mechanism is clearly (combined selectivity of 87%) predominating, but the partially selective mechanism is operative to a minor extent (13%) as well. Furthermore, the "direct ring-opening products" undergo consecutive hydrogenolysis either of endocyclic carbon–carbon bonds to open-chain decanes (OCDs) or of exocyclic carbon–carbon bonds in the alkyl side chains to methane and $C_9$ alkylcyclohexanes. The latter show again an endocyclic hydrogenolysis leading to open-chain nonanes (OCNs), and precisely the OCD and OCN isomers predicted by such a pathway were detected in the reaction product [6].

Ref. [4] also contains an evaluation of the possible improvement of the cetane number by catalytic hydroconversion. It is shown there that, in order to achieve a substantial gain in the cetane number, it is mandatory to produce OCDs with an as high as possible yield and an as low as possible degree of branching. OCD yields of up to ca. 20% were achieved on the monofunctional metallic catalysts described in Refs. [4,6].

In spite of the relatively large number of reports on ring opening of decalin on conventional bifunctional catalysts [3,7–18], such as Pt/H-Y, Pt/USY, Pt/H-Beta, Pt/H-mordenite, Pt,Ir/H-Y, or Pt,Ir/H-Beta, remarkably little is known about the maximum attainable yields of open-chain decanes. In the majority of papers, OCDs are even not mentioned as products. This is certainly due to the difficult analysis of the $C_{10}$ products which often consist of more than 100, if not 200 individual hydrocarbons. We are aware of just one paper [12], in which the maximum yield of OCDs attained from decalin on a Pt,Ir/H-Y catalyst was reported to be 4%. Our own results obtained in the decalin hydroconversion on Ir/La-X and Pt/La-X zeolites by using gas chromatographic procedures tailored for the analysis of the complex $C_{10}$ product mixtures [17] rather suggest that values around 10% are more realistic for the usually employed bifunctional catalysts with a content of noble metal around 1 wt.% and a relatively high concentration and strength of Brønsted-acid sites.

In the present communication, we wish to report on another family of bifunctional catalysts which enable ring opening of decalin with much better yields of OCDs ($Y_{OCDs} > 25\%$) than those attainable on the above-described conventional classes of catalysts. Salient features of the new catalysts are a high hydrogenolysis activity and a relatively low concentration and strength of Brønsted-acid sites.

## 2. Experimental

### 2.1. Preparation of the catalysts

The parent material for all catalysts used in this study was zeolite Beta synthesized via the dry-gel conversion (DGC) method [25,26]: 9.98 g aluminum sulfate 18 hydrate (Riedel-de Haën, grade chemically pure) were dissolved in 5.0 g demineralized water, heated to 80 °C and stirred for 30 min. Meanwhile, 69.19 g colloidal silica (Aldrich, Ludox HS40, 40 wt.% $SiO_2$ in $H_2O$), 66.84 g tetraethylammonium hydroxide solution (Sigma–Aldrich, 40 wt.%) and 12.98 g NaOH solution (4 mol $dm^{-3}$) were mixed and stirred for 30 min at room temperature. Subsequently, the two solutions were put together and stirred for another 2 h at room temperature. The resulting gel was heated to 80 °C and dried while stirring.

Approximately 1.5 g of the dry gel were placed on a porous plate inside a Teflon-lined autoclave with 2.0 g of demineralized water at the bottom [26]. The conversion was carried out at 175 °C for 48 h. Typically, such a batch resulted in 1.7 g of as-synthesized, template-containing zeolite Beta with an $n_{Si}/n_{Al}$ ratio of 14.0. After each conversion the resulting zeolite was filtered, washed with 1 $dm^3$ demineralized water and dried for at least 12 h at 80 °C in an oven. The template was removed by first heating in a nitrogen flow of 58 $dm^3$ $h^{-1}$ from room temperature to 450 °C with a heating rate of 1 °C $min^{-1}$ and holding at 450 °C for 24 h and then switching the gas to synthetic air with a flow rate of 58 $dm^3$ $h^{-1}$ and holding the temperature for another 24 h. Prior to any further modification step, ca. 3 g of the calcined zeolite Beta were slurried in 100 $cm^3$ of a 1 molar aqueous solution of sodium nitrate under stirring at 80 °C. After 4 h of stirring at 80 °C, the zeolite was filtered, washed with 1 $dm^3$ of demineralized water and dried at 80 °C. The so-prepared zeolite will be referred to as Na-Beta.

Subsequently, $Li^+$, $K^+$, $Rb^+$, or $Cs^+$ were introduced into zeolite Na-Beta by ion exchange with the corresponding chlorides. The procedure was similar to the one applied by Rabl et al. [18] for incorporating various alkali cations into zeolite Na-Y with one exception, viz. the ion exchange was conducted only once instead of four times as in Ref. [18]. 3 g Na-Beta (on a dry basis) were suspended in 100 $cm^3$ of a 1 M aqueous solution of lithium or potassium chloride or a 0.1 M solution of rubidium or cesium chloride. This is, respectively, equivalent to offering a 100- or a 10-fold excess of the ingoing cation compared to the cation-exchange capacity of the zeolite. The suspension was heated to 80 °C and stirred for 4 h. The resulting zeolite was filtered off, washed with 1 $dm^3$ of demineralized water and dried at 80 °C.

Iridium was introduced into the zeolites by ion exchange as well. The cationic complex $[Ir(NH_3)_5Cl]Cl_2$ was used. Taking into account the results of preliminary ion-exchange experiments, a 20% excess of the iridium complex was offered to the zeolite. 3 g of the alkali cation-containing zeolite were suspended in 45 $cm^3$ of demineralized water, and a solution of the calculated (vide supra) amount of $[Ir(NH_3)_5Cl]Cl_2$ in 50 $cm^3$ demineralized water was added dropwise by means of a dropping funnel within ca. 20 min under vigorous stirring at room temperature. Next, the suspension was heated to

80 °C and stirred for another 2 h. The resulting zeolite was filtered off, washed with ca. 1 $dm^3$ of demineralized water and dried at 80 °C for 12 h in an air oven. Subsequently, the iridium complex was decomposed in an air flow at 300 °C for 2 h. The resulting catalyst powder was pressed into tablets without a binder at a pressure of 127 MPa, whereupon the tablets were crushed and sieved. The particle size fraction from 0.20 to 0.32 mm was filled into the catalytic fixed-bed reactor, where the noble metal was reduced in a flow of molecular hydrogen by heating from room temperature to 360 °C with a rate of 2 °C $min^{-1}$ and holding at this temperature for two more hours. During the reduction of the noble metal dihydrogen was oxidized, whereby Brønsted acid sites were formed on the zeolite surface in a stoichiometric amount [27,28].

Note that, throughout this study, no Brønsted acid sites were generated in the Beta zeolites apart from those co-produced during the reduction of the noble metal with dihydrogen. Considering the ion-exchange capacity of zeolite Beta with an $n_{Si}/n_{Al}$ ratio of 14.0, one estimates that a maximal iridium loading of ca. 9 wt.% can be reached by the ion-exchange method described above. For the present study, two series of bifunctional Beta zeolites were prepared. One of these contained the alkali cations $Li^+$, $Na^+$, $K^+$, $Rb^+$, or $Cs^+$, about 3 wt.% of iridium, and the Brønsted acid sites co-produced during the reduction of the noble metal. Out of these five zeolites, 3.4Ir/H,Cs-Beta turned out to possess particularly attractive catalytic properties in the hydroconversion of decalin. This prompted us to prepare a second series of bifunctional catalysts containing cesium as alkali cation and different loadings of iridium in the range from 1.1 to 4.8 wt.%.

### 2.2. Characterization of the catalysts

A Varian (Vista-MPX CCD) optical spectrometer with an inductively coupled plasma (ICP-OES) was used for chemical analysis of the catalysts. The elements Si, Al, Li, Na, K, Rb, Cs, and Ir were determined after dissolution of the catalyst in a mixture of diluted hydrofluoric acid and *aqua regia*. For more details see Ref. [17].

$^{27}Al$ and $^{29}Si$ MAS NMR spectra of the hydrated zeolites (stored over a saturated aqueous sodium chloride solution at room temperature) were obtained on a Bruker MSL 400 instrument. The $^{27}Al$ MAS NMR measurements were conducted in a rotor with a diameter of 4 mm at a resonance frequency of 104.3 MHz with 800 accumulations. The spinning rate was 9 kHz. The spectra were recorded against aluminum nitrate using a pulse length of 0.61 μs and a repetition time of 0.5 s. For measuring the $^{29}Si$ MAS NMR spectra, a rotor with a diameter of 7 mm and a resonance frequency of 79.5 MHz with 380–1250 accumulations were used. Here, a spinning rate of 4.0 kHz, a pulse length of 5 μs and a repetition time of 10 s were applied. The spectra were recorded against tetramethylsilane (TMS). The program WINFIT from Bruker was used to simulate and integrate the signals.

X-ray powder diffraction patterns were recorded on a Bruker D8 Advance instrument with CuKα radiation (λ = 0.154 nm). The diffraction patterns were recorded between 2θ values of 5° and 50° with a step size of 0.02° and a step time of 0.2 s. For the determination of the noble-metal dispersion a Quantachrome Autosorb-1-C instrument was used. For the hydrogen chemisorption by static volumetry an adsorption stoichiometry of $n_H/n_{Ir} = 1$ was assumed. After the reduction treatment with the same temperature program as used in the fixed-bed reactor of the catalytic flow-type apparatus (see Section 2.1), two isotherms were measured at $T = 40$ °C. The first one was considered to be a combination of physi- and chemisorption, and the second isotherm, measured after evacuating the sample, was interpreted as physisorption only. The difference between these two isotherms was considered to be due to chemisorption only and applied for calculating the noble metal dispersion [17]. A Cambridge scanning electron microscope Cam Scan 44 at an excitation voltage of 5 kV was used to determine the morphology and the size of the zeolite crystals.

To investigate the concentration and strength of the Brønsted acid sites in the catalysts, FT-IR spectroscopic measurements with pyridine as probe molecule were applied. A Vector 22 spectrometer from Bruker with a high-vacuum sample cell was used. For the measurements the samples were pressed into very thin, rectangular self-supporting wafers, which were then placed in an IR cell with $CaF_2$ windows and a vacuum system. The metal-loaded zeolites were reduced in a flow of hydrogen at 0.1 MPa with a heating rate of 2 °C $min^{-1}$ up to 500 °C and holding for 2 h. Subsequently, the sample cell was evacuated for 4 h with a vacuum of $2.0 \times 10^{-6}$ Pa. Pyridine vapor was then introduced into the cell for 30 min with $p_{pyridine} = 3.3$ Pa. Physisorbed pyridine was removed by evacuating for 1 h at 200 °C, and a spectrum was recorded at 80 °C. The pyridine was desorbed at temperatures between $T = 200$ and 500 °C in steps of 50 °C. For the evaluation of the spectra the band of the Brønsted acid sites at 1545 $cm^{-1}$ was integrated, and the concentration $c$ of Brønsted acid sites was calculated using the following equation [29]:

$$c_{pyridine} = \frac{\bar{A} \cdot l_1 \cdot l_2}{m \cdot \varepsilon} \quad (1)$$

$\bar{A}$ stands for the integral absorption with the unit [$cm^{-1}$]; $l_1$ and $l_2$ indicate the edge lengths, and $m$ is the mass of the dry wafer, while $\varepsilon$ is the extinction coefficient. The value for $\varepsilon$ is taken from the literature [30] and is for Brønsted acid sites 1.67 cm μ$mol^{-1}$.

### 2.3. Catalytic experiments and product analysis

Throughout this study, the feed hydrocarbon was cis-decalin (Merck, purity > 98%). For its catalytic hydroconversion a high-pressure continuous-flow apparatus from stainless steel was used. Its principal parts were a saturator filled with an inert solid (Chromosorb, Merck, P/AW, 0.25–0.60 mm) impregnated with liquid cis-decalin [31], a fixed-bed reactor, and a heated product sampling device with a six-port valve allowing to introduce gaseous on-line samples of the full product into a gas chromatograph (Agilent 7890 A) equipped with a Supelco Petrocol DH 150 capillary column (150 m × 0.25 mm × 1.0 μm). Additionally, integral liquid samples of the product were collected during a run by routing the off-gas from the catalytic unit through a cooling trap held at −10 °C. These liquid product samples were stored and used for ancillary off-line analyses.

The products of catalytic hydroconversion of decalin typically consist of a very large number (viz. 100, if not 200) of individual hydrocarbons, mostly with 10 carbon atoms. We found that the Supelco Petrocol DH 150 capillary column was especially appropriate for the separation of such complex product mixtures. For assignment of the peaks in the chromatograms, a GC/MS system (Agilent 6890N coupled with a mass spectrometer Agilent 5876 B inert XL MSD) equipped with the same Supelco Petrocol DH 150 capillary column as the on-line gas chromatograph was routinely used. Besides, two-dimensional capillary gas chromatography [17] and co-injection of the reaction products with pure hydrocarbons were practiced, whenever the latter were commercially available. A related technique developed in our laboratory turned out to be particularly helpful for the assignment of peaks originating from open-chain decanes [17]: based on our prior work [32] n-decane was catalytically isomerized under different reaction conditions into mixtures of iso-decanes of known composition, and these were co-injected into the gas chromatograph with a product from decalin hydroconversion. A more detailed description of our methods for peak assignment may be found in Ref. [17].

During all catalytic experiments, the mass of dry zeolite catalyst, the hydrogen partial pressure, the partial pressure of cis-decalin

**Table 1**
Classification of the product hydrocarbons formed from decalin in this study.

| Designation | Short designation | Number of carbon atoms | Number of naphthenic rings | Molecular formula | Molar mass/g mol$^{-1}$ |
|---|---|---|---|---|---|
| Skeletal isomers | sk-Isos | 10 | 2 | $C_{10}H_{18}$ | 138 |
| Ring opening products | ROPs | 10 | 1 | $C_{10}H_{20}$ | 140 |
| Open-chain decanes | OCDs | 10 | 0 | $C_{10}H_{22}$ | 142 |
| Hydrocracked products | $C_9$- | 1–9 | [a] | [a] | [a] |

[a] Hydrocracked products are hydrocarbons with 1–9 carbon atoms, typically alkanes and one-ring naphthenes.

at the reactor entrance, and the *LHSV* amounted to 0.17–0.24 g, 5.2 MPa, 25 kPa, and 0.4–0.5 h$^{-1}$, respectively. The reaction temperature was varied from 195 to 340 °C. The quantitative evaluation of the experiments was based on the on-line analyses of the full product samples. Typically, the first of these samples was sluiced into the gas chromatograph ca. 4 h after the onset of a catalytic experiment. As in our previous investigations on bifunctional noble-metal/faujasites [16–18] and on non-acidic Ir/- and Pt/silica catalysts [6], and as reported by others [4] for Ir/γ-$Al_2O_3$, stereoisomerization of cis- into trans-decalin was by far the fastest reaction on all Ir/zeolite Beta catalysts. Hence the equilibrium between both stereoisomers (ca. 10 mole% cis-, 90 mole% trans-decalin) was established before any other reaction occurred. With this in mind, we lumped both stereoisomers into the pseudo-reactant decalin (Dec). For the calculation of the decalin conversion ($X_{Dec}$), the yields ($Y_j$) of products *j*, and their selectivities ($S_j$) see Ref. [17]. The formation of hydrocracked products with less than 10 carbon atoms will be quantitatively discussed in terms of the modified hydrocracking selectivities ($S_j^*$) which are defined as the number of moles of hydrocarbons with *j* carbon atoms formed divided by the number of moles of decalin converted into hydrocracked products [16].

In this paper, the numerous individual product hydrocarbons formed in the hydroconversion of decalin on the Ir/Beta zeolites will be classified into four groups, as listed in Table 1. Neither dehydrogenation products, such as tetralin or naphthalene, nor hydrocarbons with more than 10 carbon atoms were formed in the present investigation.

## 3. Results and discussion

### 3.1. Catalyst characterization

Chemical analysis of the ion-exchanged zeolites by ICP-OES showed that sodium was replaced quantitatively by all four alkali metals. In Table 2, the short designations of the iridium-containing Beta zeolites and their compositions as determined by ICP-OES are given. All zeolites possess an $n_{Si}/n_{Al}$ ratio of 14.0. The initial figures in the catalyst designations indicate the content of iridium in wt.% on a dry basis measured by ICP-OES. The charge-compensating cations are given in the order of their abundance. In the formulae, the subscripts after the alkali cations stand for the molar ratio of this cation to aluminum ($n_{A^+}/n_{Al}$), as determined by ICP-OES. The protons could not be determined by ICP-OES, hence the subscripts on hydrogen are calculated as the difference between unity and ($n_{A^+}/n_{Al}$).

**Table 2**
Short designations and compositions of the zeolite catalysts used in this work.

| Catalyst series | Short designation | Full formula |
|---|---|---|
| A | 3.3Ir/H,Li-Beta | 3.3Ir/$H_{0.74}$,$Li_{0.26}$-Beta |
| | 3.0Ir/Na,H-Beta | 3.0Ir/$Na_{0.53}$,$H_{0.47}$-Beta |
| | 3.2Ir/H,K-Beta | 3.2Ir/$H_{0.61}$,$K_{0.39}$-Beta |
| | 3.5Ir/Rb,H-Beta | 3.5Ir/$Rb_{0.52}$,$H_{0.48}$-Beta |
| | 3.4Ir/H,Cs-Beta | 3.4Ir/$H_{0.58}$,$Cs_{0.42}$-Beta |
| B | 4.8Ir/H,Cs-Beta | 4.8Ir/$H_{0.61}$,$Cs_{0.39}$-Beta |
| | 4.0Ir/Cs,H-Beta | 4.0Ir/$Cs_{0.53}$,$H_{0.47}$-Beta |
| | 2.0Ir/Cs,H-Beta | 2.0Ir/$Cs_{0.80}$,$H_{0.20}$-Beta |
| | 1.1Ir/Cs,H-Beta | 1.1Ir/$Cs_{0.96}$,$H_{0.04}$-Beta |

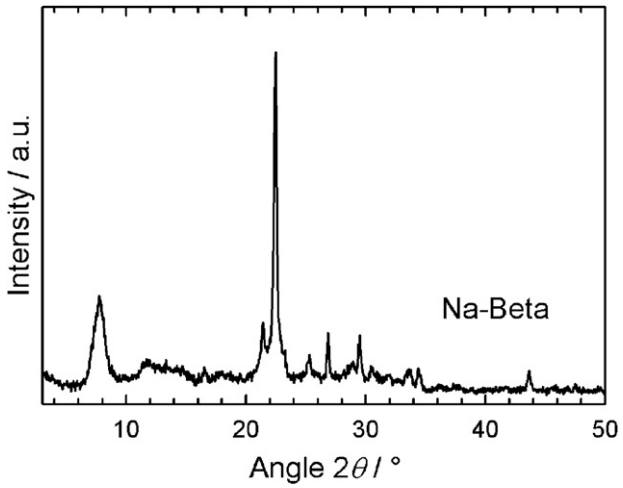


**Fig. 1.** Powder X-ray diffractogram of zeolite Na-Beta.

The powder X-ray diffractogram of zeolite Na-Beta is depicted in Fig. 1. It reveals that the sample is phase-pure. In comparison to previously measured diffractograms [26], all reflexes of zeolite Beta with high intensities are present. However, a crystalline structure was not observable in the SEM images. The zeolite rather formed agglomerates of about 5–30 μm diameter.

Shown in the Supporting Information are $^{27}$Al MAS NMR and $^{29}$Si MAS NMR spectra of the parent zeolite Na-Beta. It was found to be free from octahedrally coordinated extra-framework aluminum (no signal at 0 ppm in the $^{27}$Al MAS NMR spectrum). In addition, $^{27}$Al MAS NMR spectra were taken of the samples 3.3Ir/H,Li-Beta and 3.4Ir/H,Cs-Beta after calcination at 300 °C in an air flow. It was observed that, in both cases, a very slight dealumination of the zeolite framework had now occurred, the degree of dealumination being slightly below 5%. The $^{29}$Si MAS NMR spectrum of Na-Beta consists of four signals. Their quantitative evaluation [33] resulted in a framework $n_{Si}/n_{Al}$ ratio of 12.1, in reasonable agreement with the bulk $n_{Si}/n_{Al}$ ratio of 14.0 determined by ICP/OES.

**Table 3**
Metal dispersions of the catalysts and concentrations of pyridine adsorbed on Brønsted-acid sites at *T* = 200 °C.

| Catalyst series | Catalyst | Iridium dispersion | $n_{pyridine} \cdot m_{cat}^{-1}$/μmol g$^{-1}$ |
|---|---|---|---|
| A | 3.3Ir/H,Li-Beta | 0.18 | 189 |
| | 3.0Ir/Na,H-Beta | 0.87 | 156 |
| | 3.2Ir/H,K-Beta | 1.48 | 170 |
| | 3.5Ir/Rb,H-Beta | 0.51 | 121 |
| | 3.4Ir/H,Cs-Beta | 0.86 | 129 |
| B | 4.8Ir/H,Cs-Beta | 0.28 | 244 |
| | 4.0Ir/Cs,H-Beta | 0.41 | 172 |
| | 2.0Ir/Cs,H-Beta | 0.28 | 116 |
| | 1.1Ir/Cs,H-Beta | 0.17 | 82 |

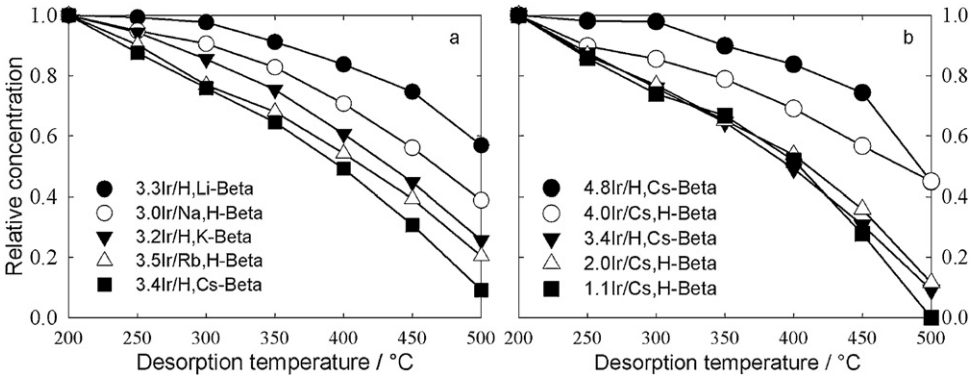


**Fig. 2.** Relative pyridine concentrations on the iridium-containing Beta zeolites determined by FT-IR spectroscopy with pyridine as probe.

Table 3 summarizes the iridium dispersions of the catalysts determined by hydrogen chemisorption and the pyridine concentrations at $T_{Des}$ = 200 °C determined by FT-IR spectroscopy. On some catalysts the dispersion seems to be surprisingly low, the reason for this is unknown. Presumably, unintended changes in the conditions of the calcination and reduction caused the low values. There is one value above unity which may be due to an adsorption stoichiometry $n_H/n_{Ir} > 1$ [34,35]. The concentrations of adsorbed pyridine on the five iridium-containing alkali Beta zeolites of series A, which are a measure of the total concentration of Brønsted acid sites, are similar. Since the Brønsted acid sites are generated via reduction of the noble metal, it is a straightforward result that, within the catalysts of series B, the measured amounts of Brønsted acid sites decrease with decreasing iridium content.

Fig. 2a and b depicts the relative concentrations of pyridine adsorbed on the catalysts at different desorption temperatures referenced to the concentration determined at 200 °C. The diminution of the relative concentration can be taken as a measure of the strength of the Brønsted acid site. At constant loading with iridium (Fig. 2a), there is a decrease in the strength of the Brønsted acid sites from the lithium- to the cesium-containing catalysts. Fig. 2b shows the decline of the relative pyridine concentration with temperature for the cesium-containing zeolites Beta with varying iridium loadings. With decreasing iridium content, the strength of the Brønsted acid sites tends to decrease. This result is in-line with the intermediate Sanderson electronegativities [36–38] which decrease from 4.13 for 4.8Ir/H,Cs-Beta to 4.00 for 1.1Ir/Cs,H-Beta.

### 3.2. General features of the hydroconversion of cis-decalin on the iridium/zeolite Beta catalysts

No deactivation was observed on any of the Ir/zeolite Beta catalysts used in this study, at least not within a time-on-stream of 36 h. Another feature that holds for all catalysts used was the rapid stereoisomerization of the cis-decalin feed into trans-decalin. On all catalysts and at all reaction temperatures the mole fraction $n_{tr\text{-}Dec}/(n_{tr\text{-}Dec} + n_{c\text{-}Dec})$ in the reactor effluent was around 0.92 (which is in all probability the equilibrium value [17]), regardless of the amount of noble metal and the decalin conversion. This is in complete agreement with what has been reported previously for cis-decalin hydroconversion on bifunctional Ir/- or Pt/La-X zeolites [17] or on Ir/- or Pt/zeolites Y containing alkali cations [18], and on non-acidic Ir/γ-$Al_2O_3$ [4] or Ir/- and Pt/silica [6]. It is very likely that the rapid stereoisomerization of cis-decalin proceeds on the noble metal via octalin intermediates, as proposed by Weitkamp [39] and Lai and Song [40].

### 3.3. Hydroconversion of decalin on the catalysts of series A (variation of the nature of the alkali cations)

Shown in Fig. 3a–e are the results of decalin hydroconversion on the five catalysts of series A. Plotted against the reaction temperature are the decalin conversion and the selectivities of the four groups of product hydrocarbons listed in Table 1. On all five catalysts the conversion starts around 200 °C, and a complete decalin conversion is reached below 300 °C. A comparison of the five conversion curves reveals that the nature of the alkali cation present in the zeolite has hardly any influence on its catalytic activity. In the decalin hydroconversion on iridium-loaded zeolite Y catalysts ($n_{Si}/n_{Al}$ = 2.4), a decline in the activity had been observed in the series from Ir/Li,Na,H-Y to Ir/Cs,Na,H-Y [18]. The lack of a pronounced influence of the nature of the alkali cations in zeolite Beta on the catalytic activity can be rationalized in terms of its much higher $n_{Si}/n_{Al}$ ratio of 14.0 and the resulting much lower concentration of charge-compensating cations. However, one could also envisage a activity of iridium on the nature of the alkali cations present in the zeolite.

Concerning the product selectivities, Fig. 3 shows a number of interesting effects. On 3.3Ir/H,Li-Beta (Fig. 3a), skeletal isomers are by far the most important products at low conversion with $S_{sk\text{-}Isos}$ = 71%. As the temperature and decalin conversion are raised, the selectivity of skeletal isomers decreases, because they are more and more consumed in consecutive reactions leading to ROPs, OCDs, and, eventually, $C_9$- hydrocarbons. In the catalyst series A the selectivities $S_{sk\text{-}Isos}$ at the lowest conversion decrease in the series from 3.3Ir/H,Li-Beta to 3.4Ir/H,Cs-Beta (from 71 to 25%). It is safely known from various sources that iridium metal lacks activity for skeletal isomerization of decalin [4–6]. The formation of skeletal isomers of decalin on the catalysts of series A must hence be ascribed to a bifunctional pathway via carbocations on the Brønsted acid sites, and the decreasing values of $S_{sk\text{-}Isos}$ in the series from 3.3Ir/H,Li-Beta to 3.4Ir/H,Cs-Beta at low conversion are completely consistent with the decreasing strength of the Brønsted acid sites in the same order (see Fig. 2).

Independent evidence for skeletal isomerization occurring on Brønsted acid sites stems from the finding that, on the catalysts of series A, spiro[4.5]decane is a major product which accounts for up to 30% of all skeletal isomers of decalin formed at low conversion. It has recently been shown that this particular isomer forms from decalin through a facile type A isomerization via carbocations [17]. Last, but not least, it should be mentioned that analogous trends were recently observed in decalin hydroconversion on iridium-loaded and alkali cation-containing faujasite catalysts [18]. The selectivity of skeletal isomers at low decalin conversion fell drastically in the series from Ir/Li,Na,H-Y to Ir/Cs,Na,H-Y, and spiro[4.5]decane, the isomer which is indicative for skeletal

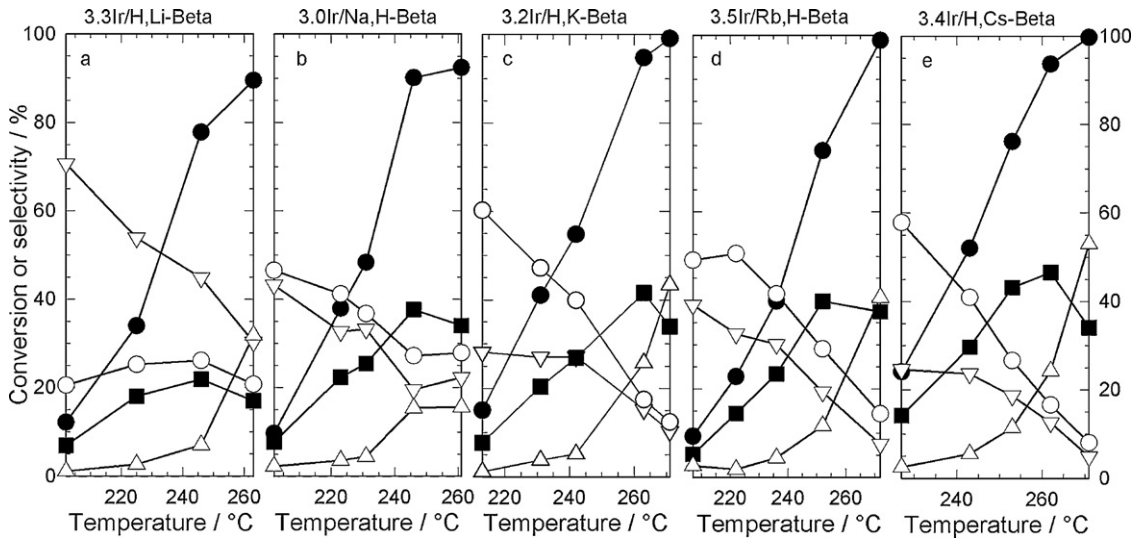


**Fig. 3.** Conversion of decalin ($X_{Dec}$, ●) and selectivities of the different groups of products ($S_{sk\text{-}Isos}$ ▽, $S_{ROPs}$ ○, $S_{OCDs}$ ■, $S_{C_9-}$ △) on the iridium-containing alkali cation-exchanged zeolites Beta (catalyst series A) at different reaction temperatures.

rearrangement occurring on Brønsted acid sites, was formed on Ir/Li,Na,H-Y and Ir/Na,H-Y only, but even not in traces on Ir/K,H-Y, Ir/Rb,Na,H-Y, and Ir/Cs,Na,H-Y [18].

The most desirable products from the viewpoint of cetane number enhancement of diesel fuel are open-chain decanes (OCDs). With all catalysts of series A, their selectivities are passing through maxima as the reaction temperature is increased (Fig. 3) reflecting that OCDs are formed by opening of the remaining ring in ROPs and, at higher severities, they are themselves consumed by consecutive hydrocracking to $C_9$- hydrocarbons. Fig. 3 also shows that the height of the maxima in the selectivities of OCDs increases markedly in the series from 3.3Ir/H,Li-Beta to 3.4Ir/H,Cs-Beta. With the latter catalyst, the maximal selectivity of OCDs is as high as 47% (Fig. 3e) which is noticeably higher than the best value reported so far in the literature for hydroconversion of decalin [18].

From an application point of view the yields of the target products are of even greater relevance than their selectivities. In Table 4 the maximum yields of open-chain decanes achieved on the five catalysts of series A are listed. All but one (3.3Ir/H,Li-Beta) fulfill the criterion for being classified as high-performance ring-opening catalysts (HIPEROCs, $Y_{OCDs,\,max.} > 25\%$). It is also seen from Table 4 that, with the zeolite Beta-based HIPEROCs, the combined yields of OCDs and ROPs reach values close to 60% and that, under the conditions of maximal OCD yields, some 20–30% of the decalin is converted into $C_9$- hydrocarbons. The 10 most important OCD isomers formed from decalin on 3.4Ir/H,Cs-Beta at $T = 262\,^{\circ}C$ and $X_{Dec} = 94\%$ were, in the order of their abundance, 4-ethyloctane, 2,6-dimethyloctane, 2,4-dimethyloctane, 2,5-dimethyloctane, 4-methylnonane, 3-methylnonane, 3,3-dimethyloctane, 3,5-dimethyloctane, 2-methylnonane, and 3,6-dimethyloctane. This enumeration shows that, as in selective ring opening of decalin on faujasitic HIPEROCs [18], mono- and dibranched OCDs with short alkyl side chains are typically formed.

For comparison, the performance data of analogous iridium-containing catalysts based on zeolite Y from our previous study [18] are also given in Table 4. There are two main differences between the catalysts based on zeolite Beta and faujasite: (i) the former are more active and give the maximum yields of OCDs at lower temperatures, and (ii) among the Beta-based catalysts, the one containing cesium as alkali cation shows the best performance, whereas sodium seems to be the best alkali cation in the faujasite-based catalysts. However, the two zeolites posses different $n_{Si}/n_{Al}$ ratios leading to similar strengths of the Brønsted acid sites after ion exchange with cesium or sodium, respectively. Also, the activity differences might in part be due to the slightly higher iridium content of the Beta zeolites.

The carbon number distributions of the hydrocracked products $C_9$- on the catalysts of series A at low to moderate yields of $C_9$- hydrocarbons are depicted in Fig. 4. The formation of large amounts of methane and $C_9$ hydrocarbons can only be rationalized in terms of a significant contribution of hydrogenolytic bond rupture on the noble metal. Superimposed to such a mechanism seems to be some bifunctional hydrocracking of $C_{10}$ naphthenes with a single ring, i.e., of ROPs, which manifests itself in an M-type distribution curve in the region $C_3$ to $C_7$ with sharp maxima at $C_4$ and $C_6$ and low $S_j^*$ values at $C_3$, $C_5$, and $C_7$. Such M-shaped carbon-number distributions

**Table 4**
Hydroconversion of decalin on iridium- and alkali cation-containing zeolites Beta (catalyst series A). Maximum yields of open-chain decanes (OCDs), combined yields of OCDs and ring-opening products (ROPs), and yields of hydrocracked products ($C_9$-). High-performance ring-opening catalysts (HIPEROCs) and the maximum yields of OCDs attained with them are bold-faced.

| Catalyst | $T_r$/°C | $X_{Dec}$/% | $S_{OCDs}$/% | $Y_{OCDs,\,max.}$/% | $Y_{OCDs,\,max.} + Y_{ROPs}$/% | $Y_{C_9-}$/% | Ref. |
|---|---|---|---|---|---|---|---|
| 3.3Ir/H,Li-Beta | 246 | 78 | 22 | 17 | 37 | 8 | This work |
| **3.0Ir/Na,H-Beta** | 246 | 90 | 38 | **34** | 59 | 19 | This work |
| **3.2Ir/H,K-Beta** | 263 | 95 | 42 | **39** | 58 | 28 | This work |
| **3.5Ir/Rb,H-Beta** | 272 | 100 | 37 | **37** | 52 | 40 | This work |
| **3.4Ir/H,Cs-Beta** | 262 | 94 | 47 | **44** | 59 | 26 | This work |
| **3.0Ir/Li,Na,H-Y** | 299 | 82 | 33 | **27** | 42 | 29 | [18] |
| **2.9Ir/Na,H-Y** | 300 | 86 | 36 | **31** | 54 | 25 | [18] |
| 2.7Ir/K,H-Y | 309 | 89 | 12 | 11 | 33 | 44 | [18] |
| 2.6Ir/Rb,Na,H-Y | 309 | 97 | 11 | 11 | 24 | 61 | [18] |
| 2.6Ir/Cs,Na,H-Y | 319 | 85 | 8 | 7 | 22 | 54 | [18] |

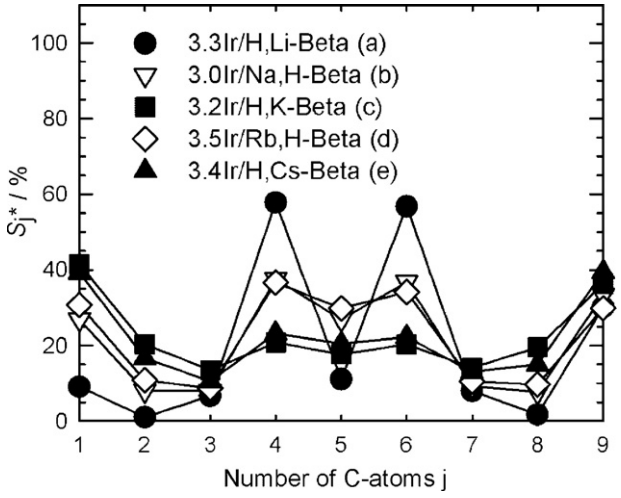


**Fig. 4.** Modified hydrocracking selectivities $S_j^*$ in the hydroconversion of decalin on iridium-containing Beta zeolites with different charge-compensating alkali cations (catalyst series A) ((a) $T_r$ = 246 °C, $X_{Dec}$ = 78%, $Y_{C_9-}$ = 8%; (b) $T_r$ = 246 °C, $X_{Dec}$ = 90%, $Y_{C_9-}$ = 19%; (c) $T_r$ = 263 °C, $X_{Dec}$ = 95%, $Y_{C_9-}$ = 28%; (d) $T_r$ = 272 °C, $X_{Dec}$ = 100%, $Y_{C_9-}$ = 40%; (e) $T_r$ = 262 °C, $X_{Dec}$ = 94%, $Y_{C_9-}$ = 26%).

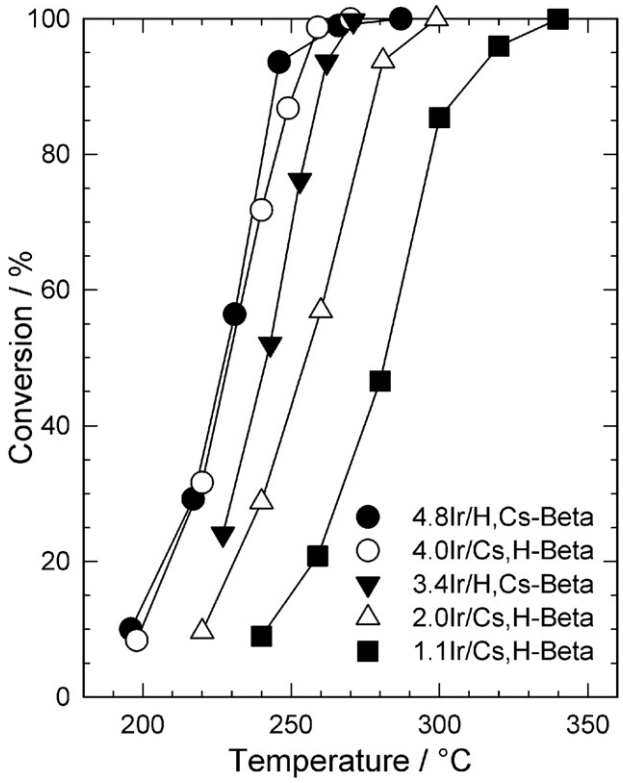


**Fig. 5.** Conversion of decalin on cesium-exchanged zeolites Beta loaded with varying amounts of iridium (catalyst series B) at different reaction temperatures.

are characteristic for the paring reaction leading mainly to isobutane and methylcyclopentane, as discussed in detail in, e.g., Ref. [17]. Indeed, on 3.3Ir/H,Li-Beta which gives the M-type curve in the most pronounced manner (Fig. 4), the $C_4$ product fraction consisted almost exclusively (95 mole%) of iso-butane, and methylcyclopentane was the main hydrocarbon (58 mole%) in the $C_6$ fraction. It is important to notice that 3.3Ir/H,Li-Beta possesses the strongest Brønsted-acid sites among the catalysts of series A (see Fig. 2a), and it gives by far the lowest yield of open-chain decanes (see Table 4). It is a reasonable conclusion that, in 3.3Ir/H,Li-Beta, there is a mismatch between the acid activity and the hydrogenolysis activity, and the too high acid strength favors the undesired paring reaction of ROPs over the desired hydrogenolytic ring opening of ROPs to OCDs. As the strength of the Brønsted acid sites of the catalysts of series A decreases from 3.3Ir/H,Li-Beta to 3.4Ir/H,Cs-Beta, the carbon-number distributions lose their pronounced M-shape, instead, nearly a plateau of $S_j^*$ appears at the carbon numbers $C_4$, $C_5$, and $C_6$. It is too early to safely interpret the occurrence of this plateau, but one could speculate that it has its origin in a consecutive hydrocracking of OCDs, either via a hydrogenolytic mechanism on iridium or via the conventional bifunctional hydrocracking mechanism via carbocations.

A detailed mechanistic view on decalin hydroconversion over iridium-containing HIPEROCs will be presented in Section 3.5.

### 3.4. Hydroconversion of decalin on the catalysts of series B (variation of the iridium content)

In Fig. 5 the conversion of decalin on the five cesium-exchanged zeolites Beta with various iridium contents are plotted in dependence of the reaction temperature. It is recalled that, as the noble metal loading increases, the concentration of Brønsted acid sites increases as well. Moreover, as Fig. 2 reveals, the strength of the Brønsted acid sites is higher for the two zeolites with the highest iridium loading, probably because the amount of cesium cations inside the zeolite is reduced. Fig. 5 clearly shows that the activity of the Ir/Cs,H-Beta zeolites increases with increasing content of noble metal up to ca. 4.0 wt.% and the concomitant increase in the acid activity.

In Fig. 6a–e the selectivities of the different product groups are shown for the same five catalysts in dependence of the reaction temperature. All Ir/Cs,H-Beta catalysts with an iridium loading of 2.0 wt.% or beyond fulfill the criterion of a HIPEROC ($Y_{OCDs,\ max.}$ > 25%), but an iridium content beyond 3.4 wt.% does not result in enhanced selectivities of OCDs. Table 5 rather reveals that catalyst 3.4Ir/H,Cs-Beta performs in an optimal manner in that it enables very favorable yields of OCDs (44%) and very high combined yields of OCDs and ROPs (59%) at the lowest yield of undesired $C_9$- hydrocarbons (26%).

The main results from Fig. 6 and Table 5 are that (i) increasing the iridium content to values beyond 3.4 wt.% does not result in catalysts with better performance and (ii) if the hydrogenolysis activity and the acid activity (concentration and strength of Brønsted acid sites) are in good balance (from ca. 2.0 to 4.0 wt.% noble metal in Ir/Cs,H-Beta), remarkably good ring-opening properties can be achieved over a relatively broad span of iridium contents.

In Fig. 7 the carbon number distributions of the $C_9$- products in terms of the modified hydrocracking selectivities $S_j^*$ are presented for the five catalysts of series B at moderate yields of hydrocracked products. The shape of these curves resembles the one obtained on the Ir/Beta zeolites containing different alkali cations (Fig. 4). In particular, large amounts of $C_1$ and $C_9$ hydrocarbons are formed which unambiguously indicates the occurrence of hydrogenolysis on the noble metal as a main hydrocracking mechanism. There is only one catalyst, namely 1.1Ir/Cs,H-Beta with the lowest iridium content, which tends to give an M-shaped distribution curve in the carbon-number range $C_3$ to $C_7$. It might well be that, at the relatively high reaction temperatures (300–320 °C) required on this catalyst with its low activity, bifunctional catalysis and the paring reaction furnish a noticeable contribution to the pathway of hydrocracking decalin. Indeed, the content of iso-butane in the $C_4$ fraction formed on this catalyst is high ($n_{i\text{-}Bu}/(n_{n\text{-}Bu} + n_{i\text{-}Bu}) = 89\%$), and so is the content of methylcyclopentane in the $C_6$ fraction ($n_{M\text{-}CPn}/n_{C_6\ \text{hydrocarbons}} = 44\%$). Note that this same catalyst was the only one in series B which failed to reach the benchmark set

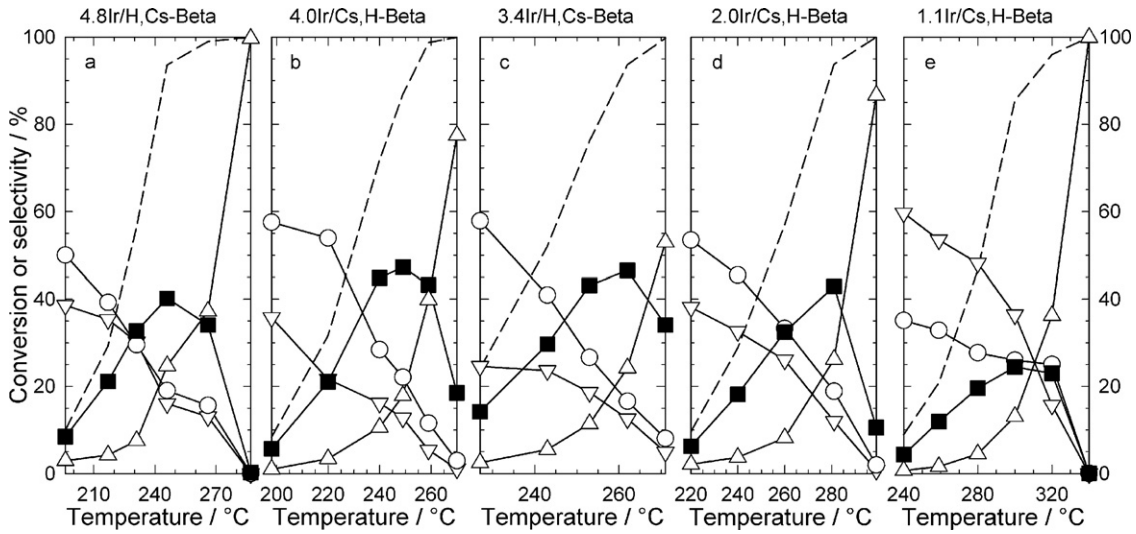


**Fig. 6.** Selectivities of the different groups of products ($S_{sk\text{-}Isos}$ ▽, $S_{ROPs}$ ○, $S_{OCDs}$ ■, $S_{C_9-}$ △) in the hydroconversion of decalin at different reaction temperatures on cesium-exchanged zeolites Beta loaded with varying amounts of iridium (catalyst series B). The dashed curves represent the decalin conversions from Fig. 5.

**Table 5**
Hydroconversion of decalin on iridium-containing Cs,H-Beta catalysts (catalyst series B). Maximum yields of open-chain decanes (OCDs), combined yields of OCDs and ROPs, and yields of hydrocracked products ($C_9$-). HIPEROCs and the maximum yields of OCDs attained with them are bold-faced.

| Catalyst | $T_r$/°C | $X_{Dec}$/% | $S_{OCDs}$/% | $Y_{OCDs,\,max.}$/% | $Y_{OCDs,\,max.} + Y_{ROPs}$/% | $Y_{C_9-}$/% |
|---|---|---|---|---|---|---|
| **4.8Ir/H,Cs-Beta** | 246 | 94 | 40 | **38** | 58 | 27 |
| **4.0Ir/Cs,H-Beta** | 259 | 99 | 43 | **43** | 55 | 39 |
| **3.4Ir/H,Cs-Beta** | 262 | 94 | 47 | **44** | 59 | 26 |
| **2.0Ir/Cs,H-Beta** | 281 | 94 | 43 | **40** | 58 | 29 |
| 1.1Ir/Cs,H-Beta | 320 | 96 | 23 | 22 | 46 | 35 |

for HIPEROCs (see Table 5). Conversely, the four other catalysts of series B, which all do fulfill the criterion of a HIPEROC (Table 5), show a common peculiarity in their carbon-number distributions of the $C_9$- products, viz. nearly a plateau at a relatively high level in the region $C_4$ to $C_6$ of the $S_j^*$ curve (Fig. 7). This very interesting feature, which was already observed with the catalysts of series A (Fig. 4), is at complete variance to monofunctional iridium catalysts lacking Brønsted acid sites. As recently demonstrated by Haas et al., hydrogenolysis of decalin on such catalysts, e.g., Ir/silica, results in hammock-type carbon-number distribution curves with virtually no $C_4$, $C_5$, and $C_6$ [6].

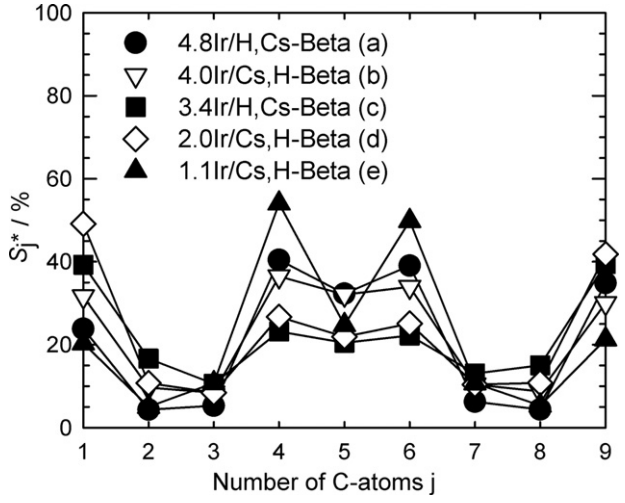


**Fig. 7.** Modified hydrocracking selectivities $S_j^*$ in the hydroconversion of decalin on iridium-containing Cs-Beta zeolites (catalyst series B) ((a) $T_r$ = 246 °C, $X_{Dec}$ = 94%, $Y_{C_9-}$ = 27%; (b) $T_r$ = 259 °C, $X_{Dec}$ = 99%, $Y_{C_9-}$ = 39%; (c) $T_r$ = 262 °C, $X_{Dec}$ = 94%, $Y_{C_9-}$ = 26%; (d) $T_r$ = 281 °C, $X_{Dec}$ = 94%, $Y_{C_9-}$ = 29%; (e) $T_r$ = 320 °C, $X_{Dec}$ = 96%, $Y_{C_9-}$ = 35%).

### 3.5. The catalytic chemistry of decalin ring opening on iridium-containing HIPEROCs

High-performance ring-opening catalysts (HIPEROCs) enable the hydroconversion of decalin into open-chain decanes with high yields, the threshold being set at $Y_{OCDs}$ > 25%. The currently known HIPEROCs contain both noble-metal and Brønsted-acid sites and are thus members of the long-known family of bifunctional catalysts. They differ, however, substantially from the conventional noble-metal/zeolite catalysts used on an industrial scale in hydrocracking of vacuum gas oil [41,42] or in the isomerization of light gasoline [43]. In these conventional bifunctional catalysts, the main function of the noble metal is – beside prevention of coke formation and the concomitant catalyst deactivation – to promote the rapid interconversion of alkanes and alkenes by dehydrogenation/hydrogenation [44,45], whereas the second principal reaction catalyzed by noble metals, i.e., hydrogenolytic cleavage of carbon–carbon bonds [19,46], is mostly undesired. Consequently, noble metals with a relatively low activity for hydrogenolysis, such as palladium or platinum, have been traditionally used in conventional bifunctional catalysts, and the content of noble metal is low, typically below 1 wt.% [47,48]. At the same time, the concentration and strength of the Brønsted-acid sites in these catalysts are relatively high, since these sites promote the desired reactions, namely skeletal rearrangements and carbon–carbon bond cleavage via β-scission of carbocations [45,49]. In contrast to these conventional bifunctional catalysts, features of HIPEROCs include

(i) a noble metal with a high activity for hydrogenolysis, e.g., iridium,

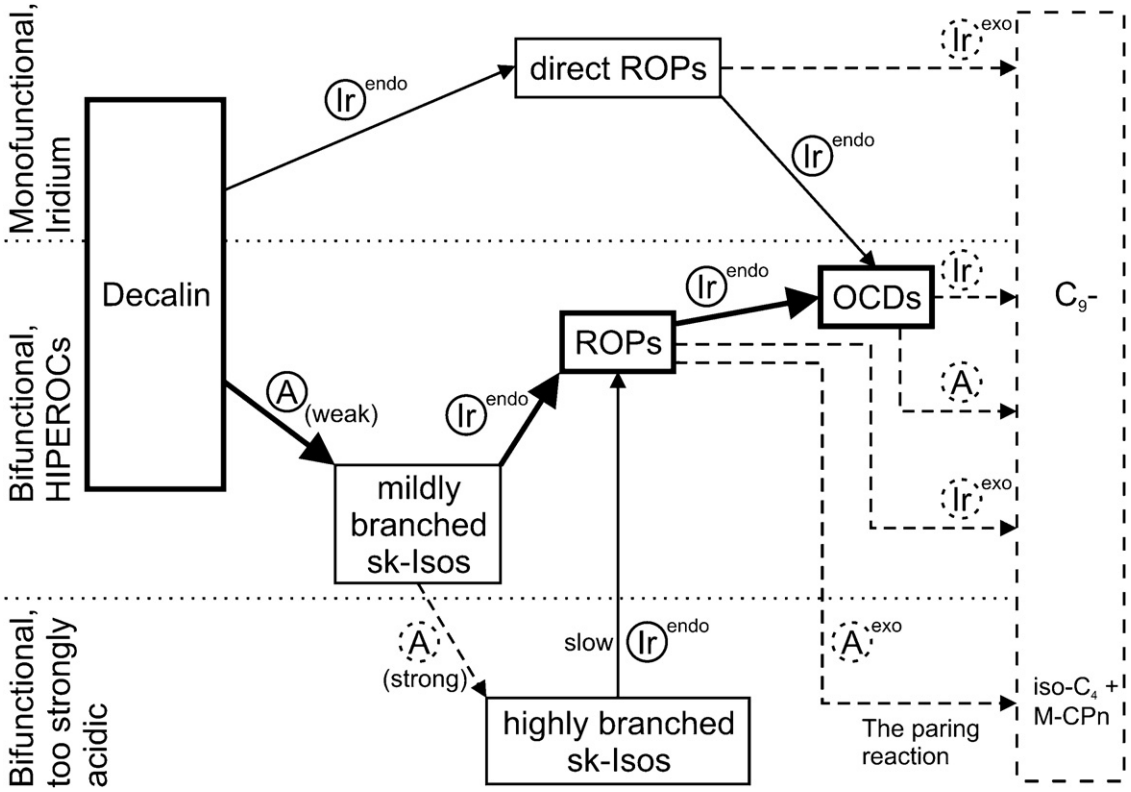


**Fig. 8.** Proposed reaction scheme for ring opening of decalin to open-chain decanes (OCDs) on HIPEROCs (bold-faced arrows in the center part of the figure). A stands for Brønsted-acid sites. Dashed arrows represent undesired reactions, *endo* and *exo* denote, respectively, hydrocracking of endocyclic and exocyclic carbon–carbon bonds. Also sketched in the upper part of the figure is the "direct ring-opening mechanism" which has been claimed for decalin hydroconversion on monofunctional iridium catalysts lacking Brønsted-acid sites [4,6]. In the lower part of the figure, undesired side reactions are shown which are believed to occur, if the concentration and/or strength of the acid sites are too high. For details concerning *the paring reaction* of $C_{10}$ naphthenes with a single ring to iso-butane and methylcyclopentane see Refs. [17,45,52,55].

(ii) a higher metal content, e.g., in the range from ca. 2 to 4 wt.% (see Table 5), and
(iii) a lower concentration and strength of Brønsted-acid sites.

In other words and using a notion that is customary in bifunctional catalysis, the optimal balance between both types of sites is fundamentally different in HIPEROCs and in conventional bifunctional catalysts. Also important for a HIPEROC is an as high as possible selectivity for cleavage of endocyclic bonds compared to that of exocyclic carbon–carbon bonds in alkyl side chains, because only the former results in the desired ring opening with retention of the carbon number.

On conventional bifunctional catalysts with their relatively low activity for hydrogenolysis and their strong acid component, cleavage of endocyclic bonds has been found to be surprisingly slow compared to β-scissions of exocyclic carbon–carbon bonds in alkyl side chains [50]. Probably, the origin of the effect is an unfavorable orbital orientation in the transition state of endocyclic β-scissions [17,45,51,52]. As a consequence, the $C_{10}$ molecules undergo extensive acid-catalyzed skeletal isomerization in the alkyl side chains followed by exocyclic β-scission, mainly into isobutane and methylcyclopentane. In fact, these are the principal $C_9$-products in decalin hydroconversion on conventional bifunctional catalysts, e.g., on 0.85Ir/La-X zeolite, while the maximum yields of the desired open-chain decanes are low, typically around 10% [17].

The direct ring opening of decalin on monofunctional iridium catalysts lacking Brønsted-acid sites is sketched in the upper part of Fig. 8. Under typical reaction conditions, it proceeds at temperatures of ca. 250–350 °C [4,6]. It is another well known fact that iridium opens five-membered rings much more readily than six-membered rings [5,21,53], hence it was proposed [4,5,21] to combine iridium-containing catalysts for decalin hydrogenolysis with a weakly acidic component, the activity of which is just sufficient for contraction of six- to five-membered rings by a so-called non-branching (or type A [45]) isomerization via carbocations. Indeed, such type A isomerizations are known to be among the fastest hydrocarbon reactions in bifunctional catalysis [45,54]. Independent evidence for an acid-catalyzed ring contraction step preceding ring opening on the iridium-containing HIPEROCs stems from the facts that (i) skeletal isomerization of decalin does occur on these catalysts (see Figs. 3 and 6), (ii) ring opening of decalin proceeds at temperatures of ca. 200–275 °C, which is significantly lower than the temperatures required for the same reaction on monofunctional iridium catalysts [4,6], and (iii) spiro[4.5]decane was undoubtedly identified as a primary product from decalin on the HIPEROCs (see Section 3.3.), at variance to direct ring opening on monofunctional iridium catalysts, where no spiro[4.5]decane at all is formed [6].

Next, the mildly branched skeletal isomers with a five-membered ring undergo ring opening to ROPs. Considering the high hydrogenolysis activity of iridium, the high metal content of HIPEROCs, their relatively low concentration and strength of Brønsted acid sites, and the reluctance of endocyclic bonds to undergo cationic β-scissions [45,52], we believe that this ring-opening step occurs predominantly, if not exclusively, by hydrogenolysis on the metal. Fig. 9 provides a more detailed view on the ring-opening step as it is believed to occur on iridium-containing HIPEROCs. Both direct ring opening of decalin, as it has been found to happen on iridium catalysts lacking Brønsted-acid sites [4,6], and opening of the five-membered ring in skeletal isomers of decalin are likely to

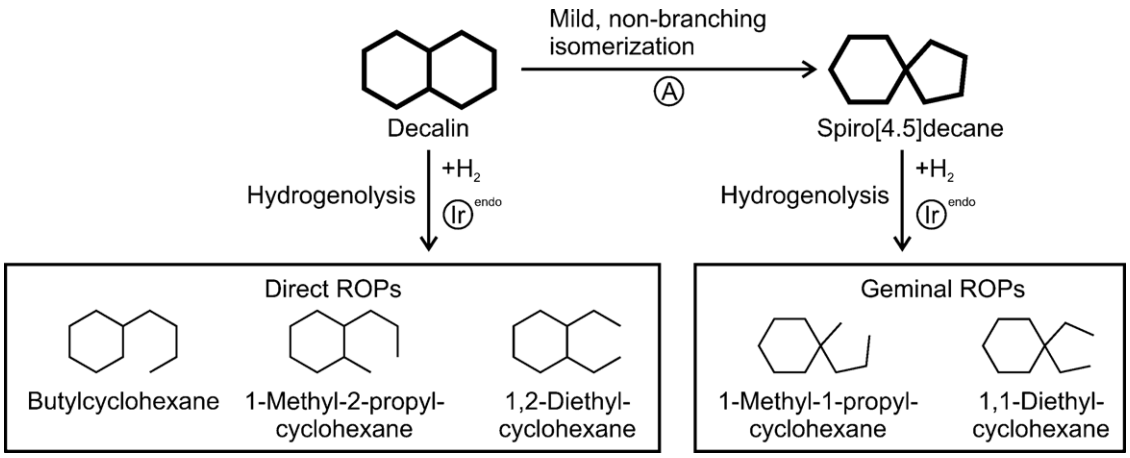


**Fig. 9.** Proposed pathways of decalin ring opening on iridium-containing HIPEROCs. Both direct ring opening of decalin (left-hand path [4,6]) and opening of the five-membered rings in skeletal isomers such as spiro[4.5]decane (right-hand path) are believed to occur. A stands for Brønsted-acid sites.

take place. A detailed look at the experimental distribution of the ROPs formed on the catalysts used in this investigation supports this view (Table 6). At low conversions, the direct ROPs butylcyclohexane, cis- and trans-1-methyl-2-propylcyclohexane, and cis- and trans-1,2-diethylcyclohexane are formed, but with selectivities that are about one half of those measured on iridium catalysts lacking Brønsted-acid sites [6]. In addition, the characteristic geminal ROPs 1-methyl-1-propylcyclohexane and 1,1-diethylcyclohexane occur which are predicted to form by hydrogenolytic cleavage of the five-membered ring in spiro[4.5]decane according to the selective (dicarbene) mechanism.

If one bears in mind that iridium preferentially cleaves bonds between unsubstituted carbon atoms (according to the selective or dicarbene mechanism), an as low as possible degree of branching in the skeletal decalin isomers favorably influences the rate of ring opening. Conversely, if the acid activity of the bifunctional catalyst is too high compared to its hydrogenolysis activity, more highly branched skeletal isomers of decalin will form (see lower part of Fig. 8) offering less unsubstituted endocyclic carbon–carbon bonds, and this will slow down the hydrogenolytic ring opening of sk-Isos to ROPs [5,21,53].

In a consecutive step, the remaining ring in ROPs is opened (Fig. 8), whereby open-chain decanes (OCDs) result, the most desired products of decalin hydroconversion. Following the same line of arguing as in the discussion of the first ring-opening step, we consider it reasonable to assume that, on HIPEROCs, endocyclic hydrogenolysis is the mechanism of making OCDs from ROPs, too. However, competing with the desired ring opening are two undesired reactions of ROPs (see Fig. 8) which both lead directly to $C_9$-hydrocarbons:

(i) One is the hydrogenolysis of exocyclic carbon–carbon bonds in the alkyl side chain(s) of the ROPs. It is evident from Fig. 8 that, for selective ring opening of decalin to occur, a hydrogenolysis component in the catalyst and reaction conditions are needed which favor as much as possible cleavage of endocyclic over that of exocyclic carbon-carbon bonds – a point which deserves particular attention in future research!

(ii) The other one is the "paring reaction" which is acid-catalyzed and consists of a series of skeletal type A (non-branching) and type B (branching) rearrangement steps followed by a rapid type A β-scission of α,γ,γ-tribranched carbenium ions [17,45,52,55]. Starting from any $C_{10}$ one-ring naphthene, it leads to the products iso-butane and methylcyclopentane. If OCDs are the desired products, the paring reaction has to be suppressed to the maximum possible extent by reducing the concentration and/or strength of the Brønsted-acid sites of the catalyst. The occurrence of the paring reaction or not can be easily monitored by measuring the carbon-number distribution of the $C_9$- products: If the paring reaction is involved, M-shaped distribution curves result in the region $C_3$ to $C_7$ with sharp maxima at $C_4$ and $C_6$, as demonstrated, for example, in Ref. [17] for decalin hydroconversion on Ir/La-X zeolite. In the present study, we perceived similar, though less pronounced M-shaped distribution curves for two catalysts, namely 3.3Ir/H,Li-Beta (Fig. 6) and 1.1Ir/Cs,H-Beta (Fig. 7) which both failed to reach the benchmark set for HIPEROCs ($Y_{OCDs,\,max.} > 25\%$). In the light of the reaction scheme depicted in Fig. 8, this failure can be attributed, respectively, to a too high acid strength and a too low hydrogenolysis activity.

**Table 6**
Comparison of the ring-opening products obtained in the hydroconversion of decalin on the catalysts of series A and B and comparison with the results obtained on two iridium catalysts lacking Brønsted-acid sites [6]. HIPEROCs are printed bold-faced.

| Series | Catalyst | $T_r$/°C | $X_{Dec}$/% | $S_{direct\ ROPs}/S_{ROPs}$/% | $S_{geminal\ ROPs}/S_{ROPs}$/% | Ref. |
|---|---|---|---|---|---|---|
| A | 3.3Ir/H,Li-Beta | 202 | 12 | 46 | 7 | This work |
| | **3.0Ir/Na,H-Beta** | 202 | 9 | 41 | 36 | This work |
| | **3.2Ir/H,K-Beta** | 213 | 15 | 56 | 32 | This work |
| | **3.5Ir/Rb,H-Beta** | 207 | 9 | 48 | 39 | This work |
| | **3.4Ir/H,Cs-Beta** | 227 | 24 | 45 | 33 | This work |
| B | **4.8Ir/H,Cs-Beta** | 196 | 10 | 31 | 47 | This work |
| | **4.0Ir/Cs,H-Beta** | 198 | 8 | 36 | 45 | This work |
| | **2.0Ir/Cs,H-Beta** | 220 | 10 | 42 | 45 | This work |
| | 1.1Ir/Cs,H-Beta | 240 | 9 | 32 | 41 | This work |
| | 0.77Ir/silica | 290 | 12 | 96 | 0 | [6] |
| | 2.59Ir/silica | 250 | 17 | 96 | 0 | [6] |

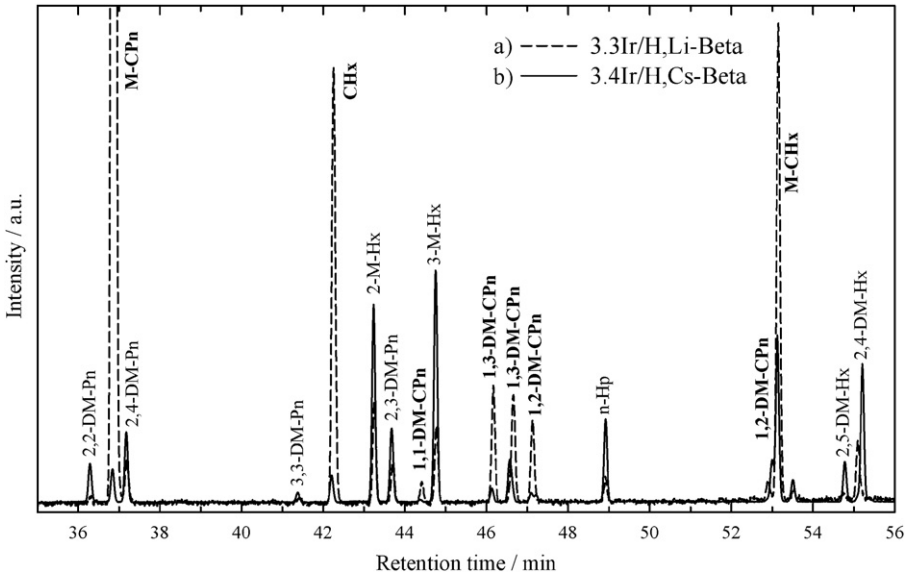


**Fig. 10.** Section of two gas chromatograms of the $C_7$ product fractions formed in the hydroconversion of decalin on (a) 3.3Ir/H,Li-Beta at $T_r$ = 246 °C and $Y_{C_9-}$ = 8% and (b) the HIPEROC 3.4Ir/H,Cs-Beta at $T_r$ = 262 °C and $Y_{C_9-}$ = 26% (C: cyclo; DM: dimethyl; Hp: heptane; Hx: hexane; M: methyl; Pn: pentane).

The proposed reaction scheme (Fig. 8) suggests that there are two principal precursors for the formation of hydrocracked products ($C_9$-), viz. ROPs or OCDs. In the case of $C_9$- formation from ROPs, regardless of whether it occurs by hydrogenolysis on iridium or via bifunctional catalysis (i.e., the paring reaction), one expects the $C_9$- hydrocarbons to consist of equal moles of alkanes and naphthenes (assuming that there is no consecutive ring opening of the $C_9$- naphthenes formed); by contrast, in the case of an exclusive $C_9$- formation from OCDs, the scheme in Fig. 8 predicts the $C_9$- hydrocarbons to consist of alkanes exclusively.

The two chromatograms of the $C_7$ fractions presented in Fig. 10 convincingly demonstrate that, at moderate yields of $C_9$-, much more $C_7$ naphthenes are formed on 3.3Ir/H,Li-Beta, whereas $C_7$ alkanes predominate in the product obtained on the HIPEROC 3.4Ir/H,Cs-Beta. This independent finding confirms and underlines that OCDs play an important role as precursors of $C_9$- hydrocarbons in decalin hydroconversion on HIPEROCs, whereas ROPs seem to be the main precursors of $C_9$- hydrocarbons on conventional bifunctional catalysts.

Finally, the reaction scheme in Fig. 8 implies that the steady-state concentration of skeletal isomers of decalin will be high, if the catalyst possesses a relatively high acid activity and a low activity for ring opening. Conversely, if the acid activity is low and the ring-opening activity by hydrogenolysis is high, the steady-state concentration of OCDs is expected to be high. A plot of $Y_{OCDs,\,max.}$ versus $Y_{sk\text{-}Isos,\,max.}$ is shown in the Supporting Information for all 9 catalysts used in the present study. It suggests that the expected correlation exists indeed.

## 4. Conclusions

The naphthenic rings in decalin, a model hydrocarbon for hydrogenated polynuclear aromatics, can be opened with unprecedented selectivities and yields of open-chain decanes (OCDs) on properly modified zeolites Beta as catalysts. With increasing reaction temperature and decalin conversion, the selectivities and yields of OCDs are passing through maxima, reflecting that the formation of OCDs occurs via skeletal isomers of decalin (sk-Isos) and one-ring naphthenes with 10 carbon atoms (ROPs) as intermediates, and they are consumed by consecutive hydrocracking reactions to hydrocarbons with less than 10 carbon atoms ($C_9$-). For example, on 3.4Ir/H,Cs-Beta with an $n_{Si}/n_{Al}$ ratio of 14, $H^+$ and $Cs^+$ as cations compensating the negative framework charges, and loaded with 3.4 wt.% of iridium, the maximum selectivities and yields of OCDs were 47% and 44%, respectively. To our knowledge, this is the best result ever reported for the selective ring opening of decalin. The OCDs formed consist mainly of mono- and dibranched iso-decanes with short alkyl (methyl and ethyl) side chains.

We propose to refer to such catalysts, which allow one to produce open-chain decanes from decalin with yields greater than 25%, as *High-Performance Ring-Opening Catalysts* (HIPEROCs). Salient features of HIPEROCs are a large-pore zeolite, e.g., Beta, with Brønsted-acid sites of a relatively low concentration and strength and a component with a high activity for hydrogenolysis of endocyclic carbon–carbon bonds, e.g., iridium. The main function of the acid catalyst component seems to be a non-branching isomerization of the feed molecules, i.e., a contraction of their six-membered into five-membered naphthenic rings which are much more readily opened by hydrogenolysis on the noble metal. It appears that, on HIPEROCs, hydrogenolysis is the predominating mechanism of ring opening. If the activity of the acid sites of the catalyst is too high (too high concentration and/or strength of the Brønsted-acid sites), the very undesired paring reaction will dominate, i.e., deep isomerization of $C_{10}$ naphthenes containing one naphthenic ring (ROPs) followed by β-scission of carbocations in alkyl side chains, and lead to a degradation of the carbon number at the level of ROPs, thereby preventing the formation of OCDs. For monitoring the occurrence or not of the paring reaction, we recommend measuring the carbon number distribution of the $C_9$- products: If the paring reaction plays a significant role, an M-shaped distribution curve will be obtained in the region of $C_3$ to $C_7$ with sharp maxima at $C_4$ and $C_6$, as shown for example for 3.3Ir/H,Li-Beta in Fig. 4, and large amounts of isobutane and methylcyclopentane will be formed.

Another possibility for detecting the occurrence of the paring reaction is a detailed analysis of the individual $C_7$ hydrocarbons formed in the hydrocracked products (Fig. 10). Much more $C_7$ naphthenes are formed, if the paring reaction plays a significant role, whereas the desired ring opening of ROPs to OCDs on a HIPEROC is accompanied by a prevailing formation of alkanes in the $C_7$ product fraction, in agreement with the reaction scheme proposed in Fig. 8.

Preparation of a HIPEROC requires a careful tuning of the Brønsted-acid activity with the hydrogenolytic activity. A convenient tool for influencing the strength of the Brønsted-acid sites in a zeolite catalyst is the variation of the nature of the charge-compensating cations, as demonstrated in this paper for zeolite Beta and in a preceding communication for faujasites [18].

## Acknowledgement

We are grateful to Professor Michael Hunger for the measurement and interpretation of the MAS NMR spectra.

## Appendix A. Supplementary data

Supplementary data associated with this article can be found, in the online version, at http://dx.doi.org/10.1016/j.apcata.2013.01.020.

## References

[1] R.C. Santana, P.T. Do, M. Santikunaporn, W.E. Alvarez, J.D. Taylor, E.L. Sughrue, D.E. Resasco, Fuel 85 (2006) 643–656.
[2] D. Kubička, N. Kumar, P. Mäki-Arvely, M. Tiitta, V. Niemi, T. Salmi, D.Y. Murzin, J. Catal. 222 (2004) 65–79.
[3] M. Santikunaporn, J.E. Herrera, S. Jongpatiwut, D.E. Resasco, W.E. Alvarez, E.L. Sughrue, J. Catal. 228 (2004) 100–113.
[4] R. Moraes, K. Thomas, S. Thomas, S. van Donk, G. Grasso, J.-P. Gilson, M. Houalla, J. Catal. 286 (2012) 62–77.
[5] G.B. McVicker, M. Daage, M.S. Touvelle, C.W. Hudson, D.P. Klein, W.C. Baird Jr., B.R. Cook, J.G. Chen, S. Hantzer, D.E.W. Vaughan, E.S. Ellis, O.C. Feely, J. Catal. 210 (2002) 137–148.
[6] A. Haas, S. Rabl, M. Ferrari, V. Calemma, J. Weitkamp, Appl. Catal. A: Gen. 425–426 (2012) 97–109.
[7] M.A. Arribas, J.J. Mahiques, A. Martínez, in: A. Galarneau, F. Di Renzo, F. Fajula, J. Védrine (Eds.), Zeolites and Mesoporous Materials at the Dawn of the 21st Century, Studies in Surface Science and Catalysis, vol. 135, Elsevier, Amsterdam, 2001 (CD-ROM 26-P-13).
[8] M.A. Arribas, A. Martínez, G. Sastre, in: R. Aiello, G. Giordano, F. Testa (Eds.), Impact of Zeolites and Other Porous Materials on the New Technologies at the Beginning of the New Millennium, Studies in Surface Science and Catalysis, vol. 142, Part B, Elsevier, Amsterdam, 2002, pp. 1015–1022.
[9] D. Kubička, N. Kumar, P. Mäki-Arvela, M. Tiitta, V. Niemi, H. Karhu, T. Salmi, D.Y. Murzin, J. Catal. 227 (2004) 313–327.
[10] N. Kumar, D. Kubička, A.L. Garay, P. Mäki-Arvela, T. Heikkilä, T. Salmi, D.Y. Murzin, Top. Catal. 52 (2009) 380–386.
[11] D. Kubička, T. Salmi, M. Tiitta, D.Y. Murzin, Fuel 88 (2009) 366–373.
[12] K. Chandra Mouli, V. Sundaramurthy, A.K. Dalai, J. Mol. Catal. A: Chem. 304 (2009) 77–84.
[13] K. Chandra Mouli, A.K. Dalai, Appl. Catal. A: Gen. 364 (2009) 80–86.
[14] H. Vuori, R.J. Silvennoinen, M. Lindblad, H. Österholm, A.O.I. Krause, Catal. Lett. 131 (2009) 7–15.
[15] D. Kubička, M. Kangas, N. Kumar, M. Tiitta, M. Lindblad, D.Y. Murzin, Top. Catal. 53 (2010) 1438–1445.
[16] J. Weitkamp, S. Rabl, A. Haas, M. Ferrari, V. Calemma, OIL GAS Europ. Magazine 37 (2) (2011) 94–98.
[17] S. Rabl, A. Haas, D. Santi, C. Flego, M. Ferrari, V. Calemma, J. Weitkamp, Appl. Catal. A: Gen. 400 (2011) 131–141.
[18] S. Rabl, D. Santi, A. Haas, M. Ferrari, V. Calemma, G. Bellussi, J. Weitkamp, Microporous Mesoporous Mater. 146 (2011) 190–200.
[19] F.G. Gault, in: D.D. Eley, H. Pines, P.B. Weisz (Eds.), Advances in Catalysis, vol. 30, Academic Press, New York, 1981, pp. 1–95.
[20] F. Weisang, F.G. Gault, J. Chem. Soc., Chem. Commun. (1979) 519–520.
[21] M. Daage, G.B. McVicker, M.S. Touvelle, C.W. Hudson, D.P. Klein, B.R. Cook, J.G. Chen, S. Hantzer, D.E.W. Vaughan, E.S. Ellis, in: A. Galarneau, F. Di Renzo, F. Fajula, J. Védrine (Eds.), Zeolites and Mesoporous Materials at the Dawn of the 21st Century, Studies in Surface Science and Catalysis, vol. 135, Elsevier, Amsterdam, 2001 (CD-ROM 26-O-04).
[22] WO 97/09290 A1, M. Touvelle, G.B. McVicker, M. Daage, S. Hantzer, C.W. Hudson, D.P. Klein, D.E.W. Vaughan, E. Ellis, J.G. Chen (Inventors), assigned to Exxon Research and Engineering Co., March 13, 1997.
[23] US Patent 5 763 731, G.B. McVicker, M. Touvelle, C.W. Hudson, D.E.W. Vaughan, M. Daage, S. Hantzer, D.P. Klein, E.S. Ellis, B.R. Cook, O.C. Feeley, J.E. Baumgartner (Inventors), assigned to Exxon Research and Engineering Co., June 9, 1998.
[24] WO 02/08158 A1, W.C. Baird Jr., J.G. Chen, G.B. McVicker (Inventors), assigned to Exxon Research and Engineering Co., January 31, 2002.
[25] P.R.H.P. Rao, M. Matsukata, Chem. Commun. 6 (1996) 1441–1442.
[26] A. Arnold, S. Steuernagel, M. Hunger, J. Weitkamp, Microporous Mesoporous Mater. 62 (2003) 97–106.
[27] J. Weitkamp, Solid State Ionics 131 (2000) 175–188.
[28] P. Gallezot, in: H.G. Karge, J. Weitkamp (Eds.), Molecular Sieves – Science and Technology, vol. 3, Springer, Berlin, 2002, pp. 257–305.
[29] H.G. Karge, Z. Phys. Chem. 76 (1971) 133–153.
[30] C.A. Emeis, J. Catal. 141 (1993) 347–354.
[31] J. Weitkamp, R. Gläser, in: G. Ertl, H. Knözinger, F. Schüth, J. Weitkamp (Eds.), Handbook of Heterogeneous Catalysis, vol. 4, 2nd ed., Wiley-VCH, Weinheim, 2008, pp. 2045–2053.
[32] J. Weitkamp, in: J.W. Ward, S.A. Qader (Eds.), Hydrocracking and Hydrotreating, Amer. Chem. Soc. Symp. Ser., vol. 20, American Chemical Society, Washington, DC, 1975, pp. 1–27.
[33] M.A. Camblor, A. Corma, S. Valencia, Microporous Mesoporous Mater. 25 (1998) 59–74.
[34] G.B. McVicker, R.T. Baker, R.L. Garten, E.L. Kugler, J. Catal. 65 (1980) 207–220.
[35] F. Locatelli, B. Didillon, D. Uzio, G. Niccolai, J.P. Candy, J.M. Basset, J. Catal. 193 (2000) 154–160.
[36] W.J. Mortier, J. Catal. 55 (1978) 138–145.
[37] H.G. Karge, M. Hunger, H.K. Beyer, in: J. Weitkamp, L. Puppe (Eds.), Catalysis and Zeolites, Springer, Berlin, Heidelberg, New York, 1999, pp. 198–326.
[38] R.T. Sanderson, in: E.M. Loebl (Ed.), Chemical Bonds and Bond Energy, Physical Chemistry, vol. 21, 2nd ed., Academic Press, New York, 1976, 218 pp.
[39] A.W. Weitkamp, in: D.D. Eley, H. Pines, P.B. Weisz (Eds.), Advances in Catalysis, vol. 18, Academic Press, New York, 1968, pp. 1–110.
[40] W.-C. Lai, C. Song, Catal. Today 31 (1996) 171–181.
[41] J.A.R. van Veen, J.K. Minderhoud, L.G. Huve, W.H.J. Stork, in: G. Ertl, H. Knözinger, F. Schüth, J. Weitkamp (Eds.), Handbook of Heterogeneous Catalysis, vol. 6, 2nd ed., Wiley-VCH, Weinheim, 2008, pp. 2778–2808.
[42] M. Rigutto, in: J. Čejka, A. Corma, S. Zones (Eds.), Zeolites and Catalysis, vol. 2, Wiley-VCH, Weinheim, 2010, pp. 547–584.
[43] S.T. Sie, in: G. Ertl, H. Knözinger, F. Schüth, J. Weitkamp (Eds.), Handbook of Heterogeneous Catalysis, vol. 6, 2nd ed., Wiley-VCH, Weinheim, 2008, pp. 2809–2830.
[44] P.B. Weisz, in: D.D. Eley, H. Pines, P.B. Weisz (Eds.), Advances in Catalysis, vol. 13, Academic Press, New York, 1962, pp. 137–190.
[45] J. Weitkamp, ChemCatChem 4 (2012) 292–306.
[46] J.H. Sinfelt, in: D.D. Eley, H. Pines, P.B. Weisz (Eds.), Advances in Catalysis, vol. 23, Academic Press, New York, 1973, pp. 91–119.
[47] J. Scherzer, A.J. Gruia, Hydrocracking Science and Technology, Marcel Dekker, New York, 1996, pp. 1–39.
[48] C. Marcilly, Acido-Basic Catalysis, vol. 2, Editions Technip, Paris, 2006, pp. 689–696.
[49] J. Weitkamp, P.A. Jacobs, J.A. Martens, Appl. Catal. 8 (1983) 123–141.
[50] J. Weitkamp, S. Ernst, in: B. Imelik, C. Naccache, G. Coudurier, Y. Ben Taarit, J.C. Védrine (Eds.), Catalysis by Acids and Bases, Studies in Surface Science and Catalysis, vol. 20, Elsevier, Amsterdam, 1985, pp. 419–426.
[51] D.W. Brouwer, in: R. Prins, G.C.A. Schuit (Eds.), Chemistry and Chemical Engineering of Catalytic Processes, Sijthoff & Noordhoff, Alphen aan den Rijn, 1980, pp. 137–160.
[52] J. Weitkamp, S. Ernst, Catal. Today 19 (1994) 107–149.
[53] G. Bellussi, A. Haas, S. Rabl, D. Santi, M. Ferrari, V. Calemma, J. Weitkamp, Chin. J. Catal. 33 (2012) 70–84.
[54] C. Marcilly, Acido-Basic Catalysis, vol. 1, Editions Technip, Paris, 2006, pp. 223–238.
[55] G.E. Langlois, R.F. Sullivan, in: L.J. Spillane, H.P. Leftin (Eds.), Refining Petroleum for Chemicals, Advances in Chemistry Series, vol. 97, American Chemical Society, Washington, DC, 1970, pp. 38–67.